JPPIPA 12(3) (2026)

Jurnal Penelitian Pendidikan IPA

http://jppipa.unram.ac.id/index.php/jppipa/index

Seismic Characteristics of Mount Agung during the October–November 2017 Period

W.T. Baskoro[1*], I.K. Putra[1], N.N. Wendri[1], I.N. Artawan[1], V.C.W. Putri[1], S. Sismanto[2]

[1] Department of Physics, Faculty of Mathematics and Natural Science, Universitas Udayana, Denpasar, Indonesia.
[2] Department of Physics, Geophysics Laboratory, Universitas Gadjah Mada, Yogyakarta, Indonesia.

Received: December 14, 2025
Revised: February 21, 2026
Accepted: March 25, 2026
Published: March 31, 2026

Corresponding Author:
Baskoro, W.T.
winardi@unud.ac.id

DOI: 10.29303/jppipa.v12i3.13893

Abstract: Mount Agung, a prominent stratovolcano in Bali, Indonesia, exhibited a significant increase in volcanic activity between October and November 2017 after 54 years of dormancy. This study investigates the seismic characteristics of this unrest period using waveform and spectral analysis of data from three monitoring stations: Abang (ABNG), Cegi (CEGI), and Yeh Kori (YHKR). The results indicate that seismicity was dominated by intermediate-to-deep volcanic earthquakes (VA and VB types), reaching a peak on October 18, 2017, with 679 VA and 266 VB events recorded. Spectral analysis through Fast Fourier Transform (FFT) revealed dominant frequencies ranging from 3.8 to 10.1 Hz, representing brittle failure mechanisms within the rigid volcanic edifice. A critical transition was observed in late November, where discrete high-frequency events declined and were replaced by continuous volcanic tremors, signaling a shift from a closed to an open magmatic system. This "seismic lull" accompanied by tremor signals, indicates the establishment of a stable conduit, facilitating magma migration toward the surface. These findings underscore the importance of spectral characteristics and event-type transitions as vital precursors for eruptive forecasting and volcanic hazard mitigation.

Keywords: 2017 Eruption; Fast fourier transform (FFT); Mount agung; Spectral analysis; VA and VB earthquakes

Introduction

Indonesia is located at the convergence zone (subduction zone) of three major global tectonic plates, namely the Indo-Australian Plate, the Eurasian Plate, and the Pacific Plate, as well as one microplate, the Philippine Plate. This subduction system results in a continuous magma supply, which in turn enhances seismic activity within volcanic systems. Mount Agung is one of the active volcanoes in Indonesia, situated in Rendang District, Karangasem Regency, Bali Province, at coordinates 115°30′30″ East Longitude and 08°20′30″ South Latitude. Mount Agung has an elevation of 3,014 m above sea level and is classified as a stratovolcano, characterized by a large and deep summit crater with a conical morphology composed of lava and volcanic ash deposits (Lowenstern et al., 2022).

Mount Agung has a history of powerful eruptions, most notably in 1963, which followed a 120-year quiescent period. After another 54-year repose, the sudden increase in volcanic and tectonic activity in 2017 necessitated a deep dive into its seismic characteristics to understand this new phase of unrest (Nugraini et al., 2023). As the highest peak in Bali, Mount Agung's activity poses a significant threat to the surrounding region (Caudron et al., 2015; Freret-Lorgeril et al., 2022). Periodic and intensive monitoring by the Center for Volcanology and Geological Hazard Mitigation (PVMBG) is required to manage these geological hazards (Andreastuti et al., 2019; Parwita et al., 2019). Processing seismic data into waveforms and spectra allows researchers to identify earthquake types and dominant frequencies. These parameters are crucial for interpreting and predicting the physical significance of volcanic behavior, which can provide early warning

How to Cite:
Baskoro, W., Putra, I., Wendri, N., Artawan, I., Putri, V., & Sismanto, S. (2026). Seismic Characteristics of Mount Agung during the October–November 2017 Period. *Jurnal Penelitian Pendidikan IPA*, *12*(3), 313-322. https://doi.org/10.29303/jppipa.v12i3.13893

signs before an actual eruption occurs. Because Mount Agung dominates the landscape of Bali, understanding its internal magmatic processes—such as magma migration through fractures or newly formed conduits—is vital for local safety and regional disaster preparedness (Zulfakriza et al., 2020).

The recorded eruptive history of Mount Agung before the recent activity includes eruptions in 1808, which produced large volumes of ash and pumice, followed by eruptive events in 1821 and 1843 that expelled ash, sand, and pumice materials. The 1963 eruption represents the most powerful eruption experienced by Mount Agung after a quiescent period of approximately 120 years (Wright et al., 2019).

This eruption commenced on 18 February 1963 and ended on 27 January 1964. In 2017, after a repose period of about 54 years, Mount Agung was reported to experience renewed increases in volcanic and tectonic activity. Continuous seismic activity was observed from September to October 2017, culminating in an eruptive phase that began on 21 November 2017 (Fridayanti, 2022; Iguchi, 2025).

Due to the increased activity experienced by Mount Agung, intensive and periodic monitoring was required. Such monitoring has been conducted continuously by the Center for Volcanology and Geological Hazard Mitigation (PVMBG) from the Observation Post located in Rendang Village, Rendang District, Karangasem Regency. The monitoring program consists of visual observations, instrumental measurements, and documentation of seismic data (Kriswati et al., 2024; McCausland et al., 2019). These seismic data can be processed to investigate the activity and characteristics of Mount Agung during the October–November 2017 period using spectral analysis. Seismic recordings from the stations are presented in the form of waveforms. Based on the acquired waveform data, earthquake types and dominant frequencies of the signals can be identified, allowing for the interpretation and prediction of the physical significance of the associated parameters (Pritaningtyas et al., 2023).

The research is based on the theory of plate tectonics, noting that Indonesia sits at the convergence of three major plates (Indo-Australian, Eurasian, and Pacific) and the Philippine microplate. This subduction system results in a continuous magma supply, which directly enhances seismic activity within volcanic systems like Mount Agung. The study utilizes theories regarding the classification of volcanic earthquakes. Specifically, VA (deep volcanic) and VB (shallow volcanic) earthquakes are distinguished by their waveform patterns and the clarity of S-wave arrivals. Furthermore, the emergence of tremor-type signals is a theoretical indicator of magma migration from depth once a conduit to the surface has been established (Lahr et al., 1994).

The research relies on Fourier Analysis and the Fast Fourier Transform (FFT). This theory states that a complex signal can be expressed as a linear superposition of periodic signals, allowing the conversion of seismic data from the time domain to the frequency domain. This conversion is essential because analyzing signals in the frequency domain is more straightforward and efficient for identifying the dominant frequencies of volcanic events (Brigham, 1988).

Method

Seismic waves can be represented in both waveform and spectral forms, which can subsequently be used as a basis for analyzing the characteristics of a volcanic system. Waveform analysis is conducted by examining the resulting signal patterns, including the arrival time differences between P waves and S waves. This analysis enables visual discrimination of different types of seismic events (Arisalwadi et al., 2017).

Spectral analysis is performed to obtain the frequency content of volcanic tremor signals that have been previously selected and classified. This analysis is carried out using the Fast Fourier Transform (FFT) method, which converts signals from the time domain into the frequency domain. Fourier analysis states that a signal can be expressed as a linear superposition of many periodic signals. If a signal is represented by the function f(t), Fourier analysis, often referred to as the Fourier series, can be expressed as:

$$f_{(t)} = \sum_{n=1}^{N} a_0 + a_n \cos(\omega_n t) + b_n \sin(\omega_n t) \quad (1)$$

$$\omega_n = 2\pi n f = \frac{2\pi n}{T} \quad (2)$$

with, $f_{(t)}$(frequency), a_0(average values), a_n(cosinus amplitude series), b_n(sinus amplitude series), and T(period).

The Fourier transform is a method used to determine the frequency content of a signal. To obtain the frequency representation, Equation (3), referred to as the Fourier transform, is applied, whereas Equation (4), known as the inverse Fourier transform, is used to reconstruct the original signal from its frequency-domain representation (Muslim et al., 2019).

$$f_{(t)} \rightarrow F_{(\omega)} = \int_{-\infty}^{\infty} f_{(t)} e^{-i\omega t}\, dt \quad (3)$$

$$f_{(\omega)} \rightarrow f_{(t)} = \frac{1}{2\pi} \int_{-\infty}^{\infty} F_{(\omega)} e^{i\omega t}\, d\omega \quad (4)$$

The Fourier transform employed in spectral analysis aims to convert signals from the time domain into the frequency domain. Signal analysis in the time domain requires relatively extensive processing involving derivatives of the signal function, which may introduce inaccuracies in the analytical results. In contrast, signal analysis is more straightforward and efficient when performed in the frequency domain (Minakami, 1974).

The research begins with seismic data acquisition, collecting waveform recordings from the ABNG, CEGI, and YHKR monitoring stations, followed by preliminary data processing using Swarm 2.8.5 to visualize waveforms, spectra, and spectrograms. During event selection, seismic events recorded simultaneously across all stations with significant maximum amplitudes are prioritized for waveform analysis, where P-wave and S-wave arrival times are determined to classify events into Deep Volcanic (VA), Shallow Volcanic (VB), or Tectonic earthquakes. Spectral analysis is then performed by applying the Fast Fourier Transform (FFT) to convert signals into the frequency domain and identify dominant frequency peaks. This is followed by an analysis of trends and fluctuations to track daily event counts and observe the transition toward tremor signals approaching the late November eruption. Finally, the process culminates in interpretation and conclusion, defining the seismic characteristics and dominant frequency ranges—specifically the 3.8–10.1 Hz range at the YHKR station—to provide evidence of magma migration through newly formed conduits, as summarized in Figure 1 (Suparman et al., 2019).

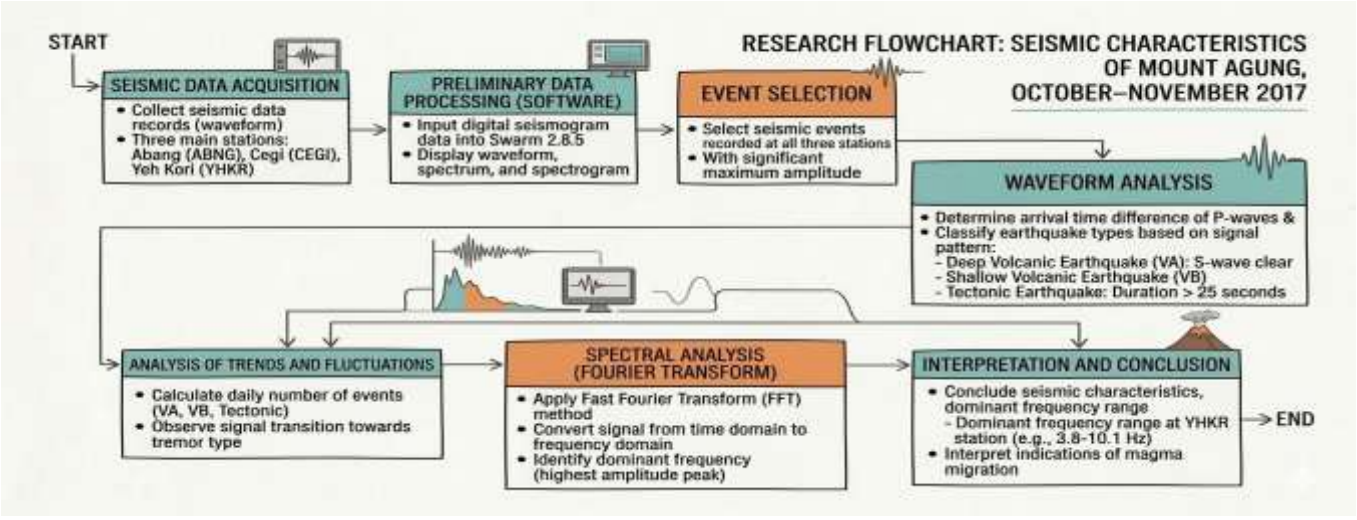

Figure 1. The flow chart for the research on the seismic characteristics of Mount Agung, Oct-Nov 2017

Results and Discussion

Data recorded by seismometers at seismic stations are displayed in the form of seismograms. These digital seismograms are processed using the Swarm 2.8.5 software, which provides waveform, spectrum, and spectrogram displays. From these seismograms, waveform and spectrogram characteristics can be examined, and spectral analysis can be performed for each event. The selected events are those that occur at approximately the same time at all three stations and exhibit maximum amplitudes on the analog seismograph, with a length of 30 mm. In the digital seismograms, these events are indicated by a red line, as shown in Figure 2. It presents only an example of waveform sampling from a seismic event. Following waveform and spectral analyses of the selected events during the October–November 2017 period at the ABNG, CEGI, and YHKR stations, the earthquake types and their dominant frequencies were determined and are summarized in Table 1. VA and VB earthquake types are distinguished based on the time difference between the arrivals of P and S waves recorded on the seismographs; when the S wave is clearly identifiable, the event is classified as a VA earthquake (Wassermann, 2011).

Events with durations exceeding 25 s are classified as tectonic earthquakes. The dominant frequency is obtained from the highest amplitude observed in the spectrum of a given event (Sahara et al., 2021). The earthquake types and their dominant frequencies recorded at the ABNG, CEGI, and YHKR stations are presented in Table 1. The data presented in Table 1 indicate that the dominant frequencies recorded at each station tend to differ. For example, a VA earthquake that occurred on 21 October 2017 at 00:08 WITA (16:08 UTC) exhibited a dominant frequency of 4.6 Hz at the ABNG station, 10.6 Hz at the CEGI station, and 10.0 Hz at the YHKR station. The corresponding earthquake waveforms are shown in Figure 3.

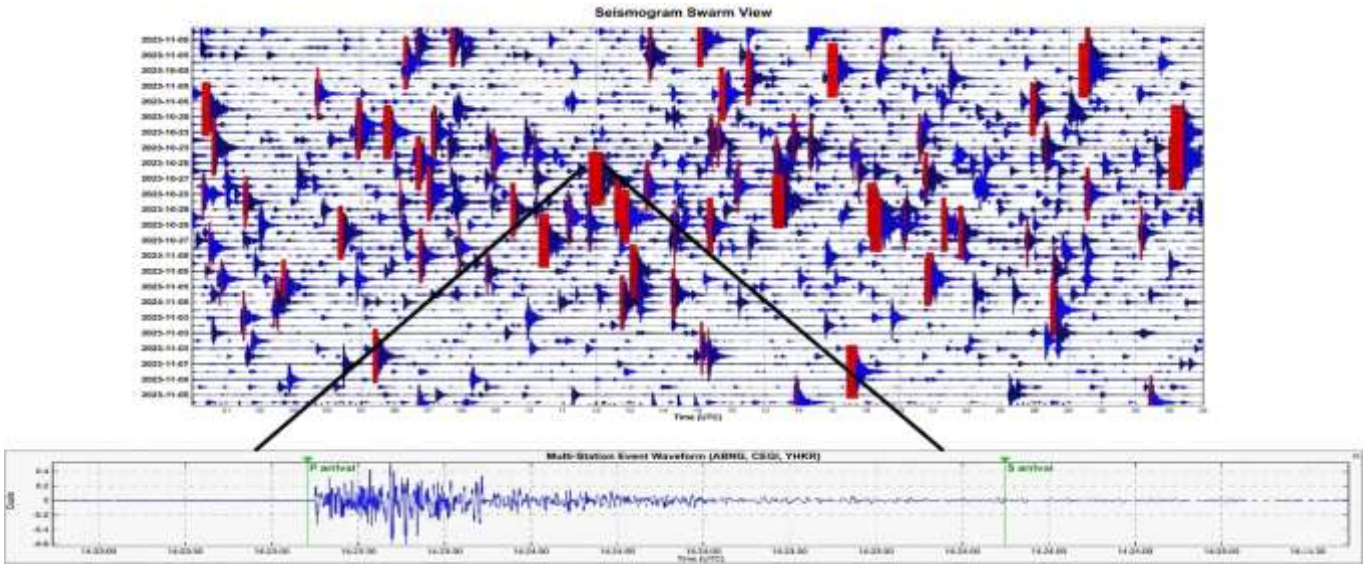

Figure 2. Sampling of a seismic event from the Mount Agung seismogram on 19 October 2017

Table 1. Earthquake Types and Their Dominant Frequencies Recorded at the ABNG(A), CEGI(C), and YHKR(Y) Stations, (DF = Dominant Frequency)

Date	Time	Earthquake Type	Stations		
			A	C	Y
			DF (Hz)	DF (Hz)	DF (Hz)
18-10-2017	16.21	VA	3.4	12.5	4.9
18-10-2017	16.47	VA	3.4	10.5	5
18-10-2017	17.00	VB	3.5	6.4	4.9
18-10-2017	17.43	VA	3.5	10.5	6.4
18-10-2017	18.21	VB	6.8	10.2	6.8
18-10-2017	22.18	VA	3.6	6.4	4.9
18-10-2017	22.26	VA	3.5	6.5	4.4
19-10-2017	00.30	VA	3.5	7	4.9
19-10-2017	00.54	VA	6.8	10	6.4
19-10-2017	02.05	VA	3.4	8.7	6.6
19-10-2017	02.29	VB	6.8	10.1	5.1
19-10-2017	04.29	VB	3.5	6.5	5
19-10-2017	05.11	VB	3.4	6.5	5
19-10-2017	06.47	VA	3.5	9.9	5.1
19-10-2017	07.20	VB	3.5	8.8	5
19-10-2017	07.42	VA	5.6	10.2	4.4
19-10-2017	08.20	VA	3.5	10	4.3
19-10-2017	09.10	VA	3.6	6.7	4.4
19-10-2017	11.13	VA	3.6	10.2	8.3
19-10-2017	11.51	VA	3.5	10	4.2
19-10-2017	13.12	VA	3.5	10.9	5.5
19-10-2017	13.55	VB	3.5	10.1	4.7
19-10-2017	16.35	VB	3.5	10.1	4.1
19-10-2017	16.45	VA	3.5	10.1	10.1
19-10-2017	17.49	Tectonic	3.5	10.7	4.6
19-10-2017	21.02	Tectonic	3.1	10.8	4.7
20-10-2017	09.48	VA	4.6	10.5	10
20-10-2017	11.37	VA	3.6	10.4	4.7
20-10-2017	12.49	Tectonic	5.4	10.4	5
20-10-2017	14.41	VA	3.6	6.9	4.8
20-10-2017	17.13	VB	5.1	10.6	4.3
20-10-2017	21.29	Tectonic	4.7	6.2	4.9
21-10-2017	00.08	VA	4.6	10.6	10
21-10-2017	01.21	VB	3.6	6.8	4.7

Date	Time	Earthquake Type	Stations		
			A	C	Y
			DF (Hz)	DF (Hz)	DF (Hz)
21-10-2017	05.05	VA	2.8	8.1	4.3
21-10-2017	07.28	VA	5.3	6.4	5.1
22-10-2017	15.54	VB	5.1	9.7	7.7
22-10-2017	23.22	VB	5.1	10.5	4.5
23-10-2017	14.06	VA	4.7	9.2	9
23-10-2017	14.29	VA	3.6	10.4	4.2
23-10-2017	23.27	VA	5	8.8	4.3
24-10-2017	03.40	VA	3.6	8	4.8
27-10-2017	16.12	VB	3.6	8.8	4.8
29-10-2017	07.56	VA	4.9	10.2	3.8
29-10-2017	08.18	Tectonic	8.5	5	4.8
29-10-2017	09.49	VA	3.7	10.5	4.3
29-10-2017	16.52	Tectonic	4.3	6.2	6.6
31-10-2017	03.09	VB	8.6	10.3	4.9
31-10-2017	11.51	VB	4.6	10.5	4.6
04-11-2017	22.42	VB	3.4	6.1	4.2
06-11-2017	07.17	VA	5.1	5.6	4.7
06-11-2017	21.15	VA	3.4	6.2	4.7
09-11-2017	09.26	VA	5.8	10	4.5
09-11-2017	13.32	VA	5.3	9.6	4.5
11-11-2017	07.01	VA	5.3	9	5
13-11-2017	09.12	VB	6.8	10.2	4.5
14-11-2017	21.15	VA	3.6	8.6	4.5
14-11-2017	21.20	VB	3.6	9.9	4.4
14-11-2017	22.43	VB	4.7	8.3	4.3
15-11-2017	08.13	VA	3.8	8.8	4.8
17-11-2017	00.48	VA	5.1	6.8	4.4
19-11-2017	22.42	VB	3.6	5.3	3.5
22-11-2017	22.29	Tectonic	8.5	10.5	5.1
27-11-2017	05.29	VA	2.8	9.2	4.7
29-11-2017	20.17	VA	4.5	7.6	5.4

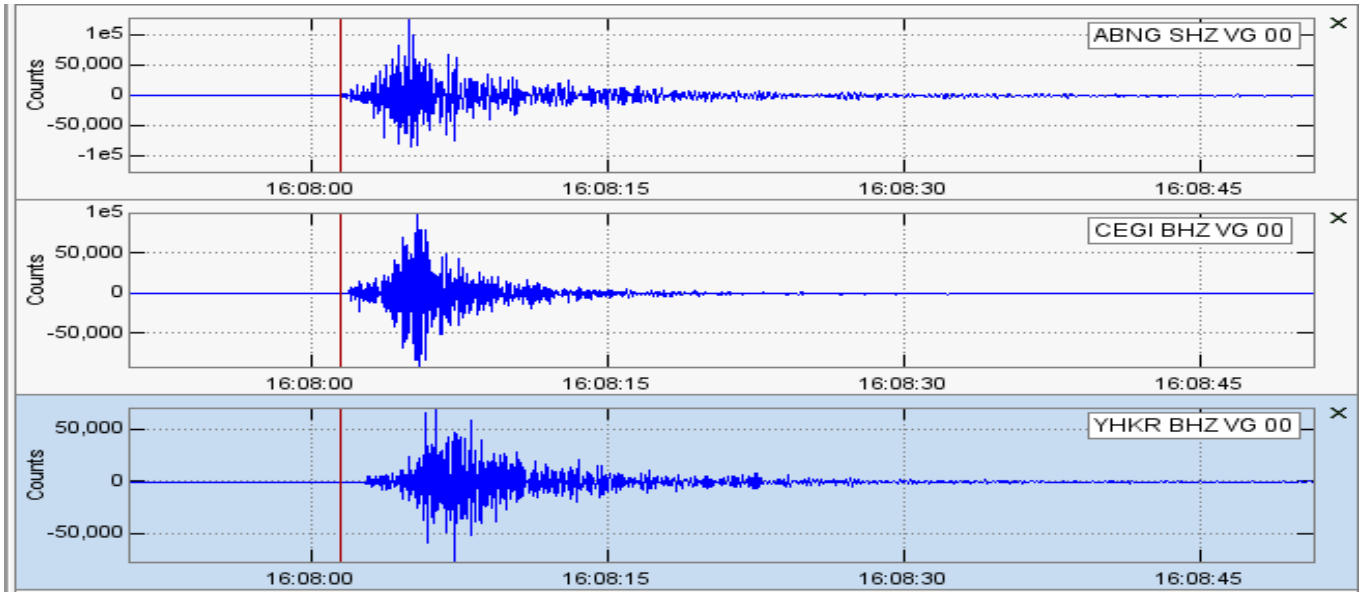

Figure 3. Waveforms of a VA earthquake recorded on 21 October 2017 at 00:08 WITA at the ABNG, CEGI, and YHKR stations

It can be inferred that the earthquake source was located closer to the ABNG and CEGI stations, resulting in a delayed arrival of the P wave at the YHKR station due to the longer travel time required to reach the seismograph. The CEGI station is located approximately 4.1 km southeast of the ABNG station. The proximity of

these two stations leads to similar seismic wave travel times. The YHKR station is situated about 4.3 km south of the active crater, whereas the ABNG station is located approximately 9.6 km northwest of the active crater. To illustrate additional differences, the spectrogram of a VA earthquake that occurred on 9 November 2017 at 09:26 WITA (01:26 UTC) is shown in Figure 4.

Based on the highest amplitudes of the events, indicated by dark red colors, the frequency content of VA earthquakes can be identified as 3–9 Hz at the ABNG station, 8–11 Hz at the CEGI station, and 4–10 Hz at the YHKR station. The waveform patterns and frequency content at the ABNG and YHKR stations tend to be similar because both stations are located at relatively comparable elevations above sea level. The elevations of the ABNG, YHKR, and CEGI stations are 1,433 m, 1,216 m, and 945 m above sea level, respectively. Because the YHKR station is located closest to the active crater compared to the ABNG and CEGI stations, and its elevation lies between those of the other two stations, the spectral analysis in this study primarily focuses on data from the YHKR station. The dominant frequency of each event can be identified from its spectrum, as shown in Figure 5 (Abidin et al., 2009).

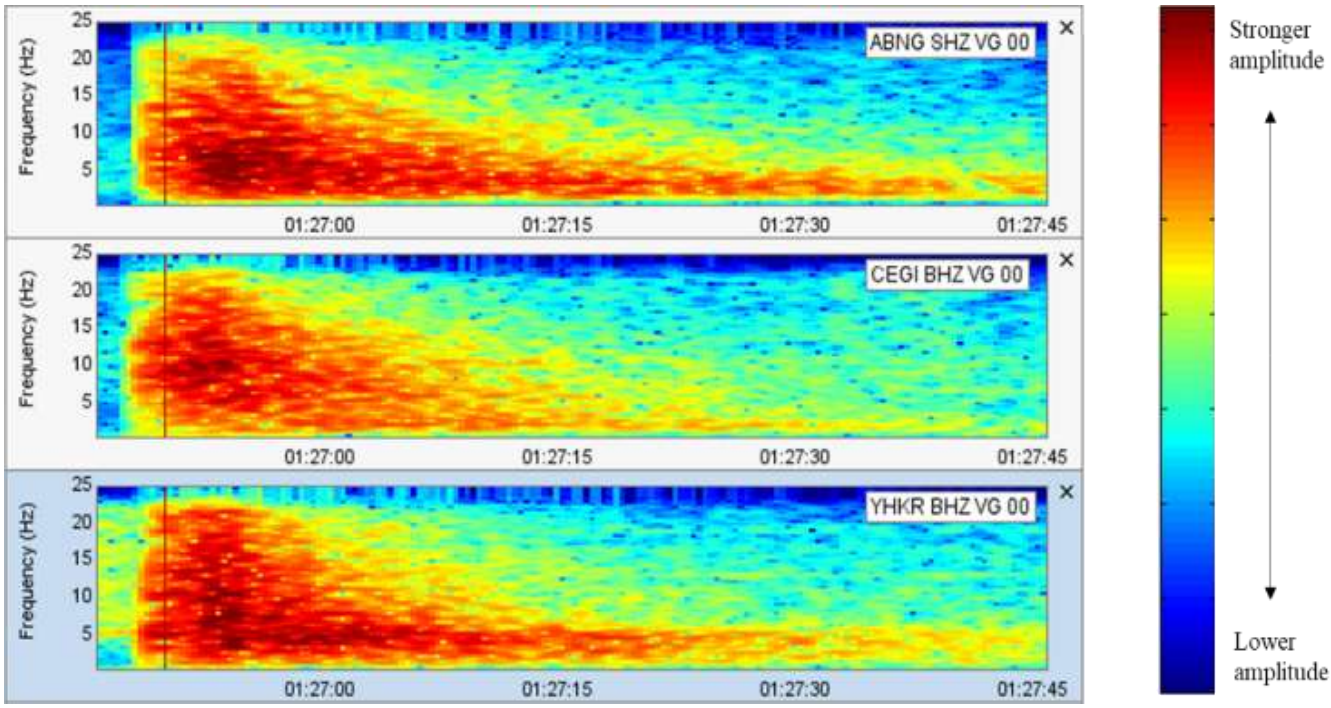

Figure 4. Spectrograms of a VA earthquake recorded on 9 November 2017 at 09:26 WITA at the ABNG, CEGI, and YHKR stations

The spectrum of a tectonic earthquake that occurred on 19 November 2017 at 22:42 WITA is shown in Figure 3. At the ABNG station, the earthquake amplitude increases and reaches its peak at a frequency of 3.6 Hz, after which it decreases over the frequency range of 3.7–10 Hz. The point of maximum amplitude represents the dominant frequency of the earthquake, which is 3.6 Hz, indicating that the strongest energy release occurred at this frequency. At the CEGI station, the earthquake amplitude exhibits more complex variations. It initially increases up to a frequency of 3.7 Hz, followed by a sharp decrease, and then gradually increases again in the range around 4.7 Hz, reaching a peak at 5.3 Hz. The amplitude then decreases sharply after 5.2 Hz before increasing again up to 7 Hz, and subsequently decreases over the frequency range of 7–12 Hz. At the YHKR station, the earthquake amplitude appears relatively constant up to a frequency of 3.1 Hz, then increases to reach its maximum amplitude at 3.5 Hz, after which the amplitude gradually decreases up to a frequency of 10 Hz.

Based on the information presented in Table 1, which summarizes the dominant frequencies of the recorded earthquakes, the dominant frequency range of VA earthquakes at the ABNG station is 2.8–6.8 Hz, while VB earthquakes exhibit dominant frequencies in the range of 3.4–8.6 Hz, and tectonic earthquakes show dominant frequencies between 3.6 and 8.5 Hz. At the CEGI station, the dominant frequencies of VA earthquakes range from 5.6 to 12.5 Hz, those of VB earthquakes from 6.1 to 10.7 Hz, and those of tectonic earthquakes from 5.0 to 10.4 Hz. Meanwhile, at the YHKR station, VA earthquakes have dominant frequencies ranging from 3.8 to 10.1 Hz, VB earthquakes from 4.1 to 6.8 Hz, and tectonic earthquakes from 3.5 to 6.6 Hz (Albino et al., 2019).

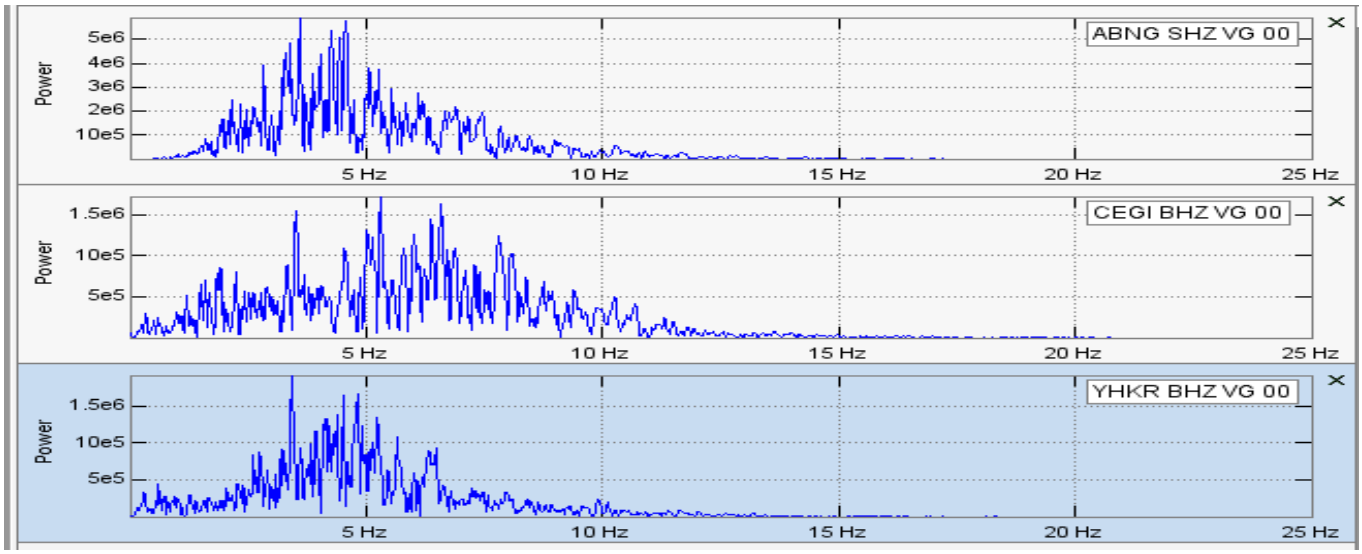

Figure 5. Spectra of a tectonic earthquake recorded on 19 November 2017 at 22:42 WITA at the ABNG, CEGI, and YHKR stations

The VA, VB, and tectonic earthquakes exhibited fluctuations before the eruption on 21 November 2017. The numbers of VA and VB earthquakes reached their maxima on 18 October 2017, with totals of 679 and 266 events, respectively. These volcanic earthquakes may indicate that magma was migrating upward by exploiting fractures or newly formed small conduits. On 19 October 2017, 113 tectonic earthquakes were recorded. These tectonic events are likely associated with fault structures between Mount Agung and Mount Batur, which trend in a northeast–southwest direction (Cho et al., 2015).

Subsequently, seismicity decreased over time in conjunction with the occurrence of eruptive activity released from the crater. The temporal decrease in VA, VB, and tectonic earthquakes is shown in Figure 6.

Tectonic earthquakes showed a sharp decrease starting on 19 October 2017, declining from 113 events to 20 events on 20 October. The number of VA and VB earthquakes also gradually decreased over time. This reduction in seismicity continued until 21 November 2017, when a volcanic ash emission reached a height of 700 m above the summit (Octavia et al., 2022). Subsequent eruptions occurred on 25, 26, and 27 November, with ash columns reaching up to 3,000 m above the summit, leading to a change in alert status from Siaga to Awas.

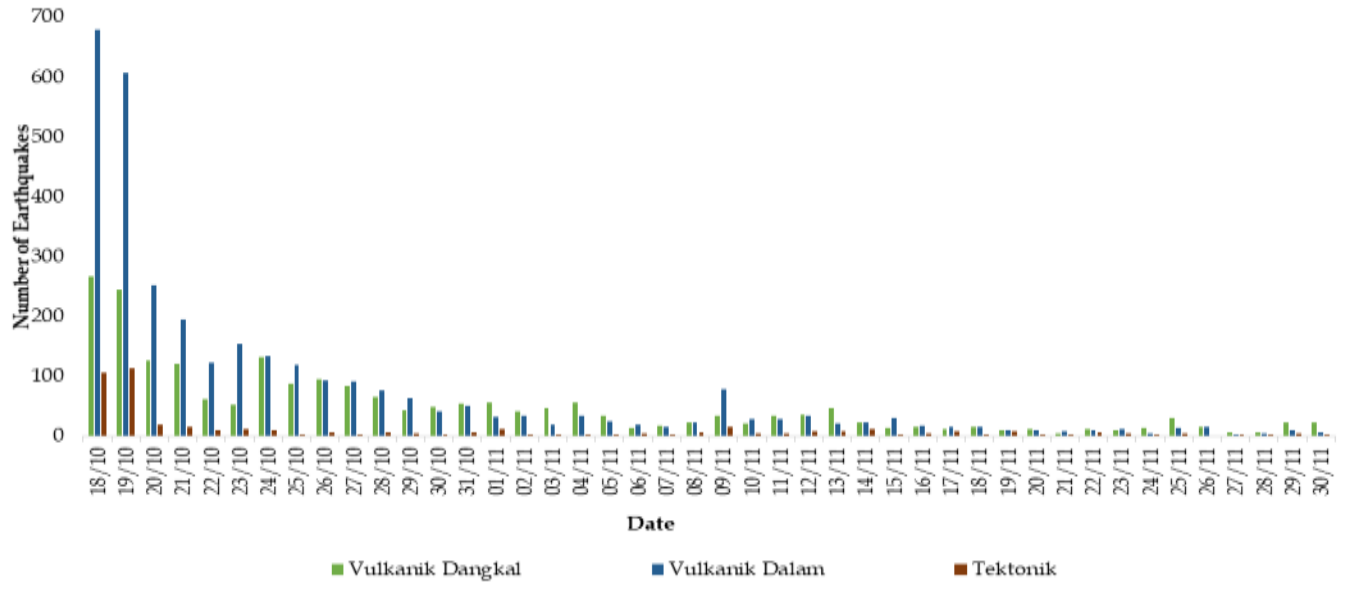

Figure 6. Fluctuations of VA, VB, and tectonic earthquakes at Mount Agung during the October–November 2017 period (McNutt et al., 2015)

On 28 November 2017, another eruption occurred with an ash column height of approximately 4,000 m above the summit. On 29 November 2017, an additional eruption was recorded, producing an ash column reaching 2,000 m above the summit. Toward the end of November, volcanic earthquakes were increasingly replaced by tremor-type signals, which may indicate magma migration from depth after a conduit to the surface had been established (Nugroho et al., 2014).

The occurrence of 113 tectonic earthquake events on October 19, 2017, immediately following the volcanic seismic peak, introduces a new dimension to understanding the dynamics of this crisis. Spatially, these earthquakes were oriented in a Northeast–Southwest direction, linking the Mount Agung system with the Batur caldera complex. This phenomenon is interpreted as a response of local geological structures to static stress transfer induced by the substantial magma volume. This aligns with the study by Albino et al. (2019), which states that massive dike intrusions beneath Agung not only trigger internal seismicity but are also capable of reactivating surrounding faults, creating a complex seismic pattern between the two neighboring volcanic systems.

Entering November, a sharp downward trend in the number of discrete earthquakes (VA and VB) was observed—a period frequently referred to as a "seismic lull." However, this decline did not signify a return to volcanic stability. On the contrary, the emergence of tremor signals, which began to dominate toward the end of November, marked the transition from a closed system to an open system. Referring to the theory by (Syahbana et al., 2019), Once the conduit has formed and become thermally primed, the rock surrounding the magma path loses its brittleness and becomes more plastic. Consequently, magmatic energy is no longer released through rock fracturing that generates VA/VB events, but rather through continuous fluid resonance (tremors) as magma migrates toward the surface (Pranata et al., 2019).

Overall, the chronological sequence from high-frequency increases (VA/VB) to low-frequency signals (tremors) provides a comprehensive overview of the 2017 Agung eruption cycle. The frequency dominance in the 3.8–10.1 Hz range serves as a physical fingerprint of Mount Agung's rigid rock, which resisted magmatic pressure before eventually yielding in late November. Understanding the transition from volcano-tectonic earthquakes to tremors is key to disaster mitigation; it demonstrates that a "quiet" period in terms of earthquake quantity may actually indicate that the magma conduit has fully opened and an eruption is imminent (Gile, 1974).

Conclusion

In summary, the seismic activity of Mount Agung during the October–November 2017 period was characterized by a dominant occurrence of VA and VB volcanic earthquakes with a dominant frequency range of 3.8 to 10.1 Hz, indicating intense brittle failure within a rigid volcanic edifice due to magmatic fluid injection. The progression of seismicity, which peaked on October 18, 2017, and was followed by a Northeast–Southwest tectonic response, underscores a significant static stress transfer that destabilized the surrounding regional faults. Furthermore, the subsequent transition from discrete high-frequency events to continuous volcanic tremors in late November serves as a critical indicator of an open-system shift, signifying that a stable magma conduit had been established. This "seismic lull" and the shift in signal characteristics provide essential forensic evidence for volcanic monitoring, demonstrating that such transitions are vital precursors to imminent eruptive activity.

Acknowledgments
We acknowledge the LPPM Universitas Udayana, Bali, for funding the 2024 Riset Unggulan program Studi. We also express our gratitude to all respondents and everyone who participated in this research.

Author Contributions
The authors' contributions to this study are as follows: Conceptualization, Baskoro, W.T. and Putri, V.C.W.; methodology, Baskoro, W.T.; software, Putra, I.K. and Wendri, N.N.; validation, Baskoro, W.T. and Sismanto, S.; formal analysis, Baskoro, W.T.; investigation, Baskoro, W.T. and Artawan, I.N.; resources, Baskoro, W.T.; data curation, Baskoro, W.T.; writing—original draft preparation, Baskoro, W.T.; writing—review and editing, Baskoro, W.T.; visualization, Baskoro, W.T.; supervision, Sismanto, S.; project administration, Wendri, N.N.; funding acquisition, Putra, I.K.

Funding
This research was funded by Lembaga Penelitian dan Pengabdian kepada Masyarakat (LPPM), Universitas Udayana, under Grant No. B/255.593/UN14.4. A/PT.01.03/2024.

Conflicts of Interest
The authors declare that there are no conflicts of interest in the conduct of this research and the preparation of this manuscript, as the study was undertaken solely for academic development and to contribute to the scientific literature.

References

Abidin, H. Z., Andreas, H., Meilano, I., Gamal, M., Gumilar, I., & Abdullah, C. I. (2009). Deformasi Koseismik dan Pascaseismik Gempa Yogyakarta 2006 dari Hasil Survei GPS. *Indonesian Journal on*

Geoscience, *4*(4), 275–284. https://doi.org/10.17014/ijog.4.4.275-284

Albino, F., Biggs, J., & Syahbana, D. K. (2019). Dyke intrusion between neighbouring arc volcanoes responsible for 2017 pre-eruptive seismic swarm at Agung. *Nature Communications*, *10*(1), 748. https://doi.org/10.1038/s41467-019-08564-9

Andreastuti, S., Paripurno, E., Gunawan, H., Budianto, A., Syahbana, D., & Pallister, J. (2019). Character of community response to volcanic crises at Sinabung and Kelud volcanoes. *Journal of Volcanology and Geothermal Research*, *382*(2), 298–310. https://doi.org/10.1016/j.jvolgeores.2017.01.022

Arisalwadi, M., Maryanto, S., & Triastuty, H. (2017). Analisis Spektral dan Waveform Cross Correlation Tremor Vulkanik Gunungapi Bromo Jawa Timur Pada Letusan Tahun 2016. *Natural B*, *4*(1), 57–64. Retrieved from https://natural-b.ub.ac.id/index.php/natural-b/article/download/388/pdf

Brigham, E. O. (1988). *The fast Fourier transform and its applications*. Prentice Hall.

Caudron, C., Syahbana, D. K., Lecocq, T., Van Hinsberg, V., McCausland, W., Triantafyllou, A., Camelbeeck, T., Bernard, A., & Surono. (2015). Kawah Ijen volcanic activity: a review. *Bulletin of Volcanology*, *77*(3), 16. https://doi.org/10.1007/s00445-014-0885-8

Cho, Y. H., Caleon, I. S., & Kapur, M. (2015). *Authentic Problem Solving and Learning in the 21st Century*. Springer Singapore. https://doi.org/10.1007/978-981-287-521-1

Freret-Lorgeril, V., Bonadonna, C., Corradini, S., Guerrieri, L., Lemus, J., Donnadieu, F., Scollo, S., Gurioli, L., & Rossi, E. (2022). Tephra characterization and multi-disciplinary determination of Eruptive Source Parameters of a weak paroxysm at Mount Etna (Italy). *Journal of Volcanology and Geothermal Research*, *421*. https://doi.org/10.1016/j.jvolgeores.2021.107431

Fridayanti, D. E. (2022). *Analisis Gempa Vulkanik Gunung Merapi Dan Korelasi Terhadap Pengukuran Infrasonik*. Universitas Islam Negeri Maulana Malik Ibrahim.

Gile, W. W. (1974). A Mercury Pendulum Seismometer. *Geophysical Journal International*, *36*(1), 153–165. https://doi.org/10.1111/j.1365-246X.1974.tb03630.x

Iguchi, M. (2025). Integrated Research on Large-Scale Eruption at Sakurajima Volcano. *Journal of Disaster Research*, *20*(2), 186–196. https://doi.org/10.20965/jdr.2025.p0186

Kriswati, E., Meilano, I., Hasib, M., Saepuloh, A., Kuncoro, H., Dewanto, B. G., & Fuadi, A. (2024). Explosion mechanism and volume estimation of volcanic ash during the eruption of Sinabung Volcano on February 19, 2018: Insight from kinematic GPS and seismic data. *Journal of Volcanology and Geothermal Research*, *447*(1), 108034. https://doi.org/10.1016/j.jvolgeores.2024.108034

Lahr, J. C., Chouet, B. A., Stephens, C. D., Power, J. A., & Page, R. A. (1994). Earthquake classification, location, and error analysis in a volcanic environment: implications for the magmatic system of the 1989–1990 eruptions at redoubt volcano, Alaska. *Journal of Volcanology and Geothermal Research*, *62*(1–4), 137–151. https://doi.org/10.1016/0377-0273(94)90031-0

Lowenstern, J. B., Wallace, K., Barsotti, S., Sandri, L., Stovall, W., Bernard, B., Privitera, E., Komorowski, J. C., Fournier, N., Balagizi, C., & Garaebiti, E. (2022). Guidelines for volcano-observatory operations during crises: recommendations from the 2019 volcano observatory best practices meeting. *Journal of Applied Volcanology*, *11*(1). https://doi.org/10.1186/s13617-021-00112-9

McCausland, W. A., Gunawan, H., White, R. A., Indrastuti, N., Patria, C., Suparman, Y., Putra, A., Triastuty, H., & Hendrasto, M. (2019). Using a process-based model of pre-eruptive seismic patterns to forecast evolving eruptive styles at Sinabung Volcano, Indonesia. *Journal of Volcanology and Geothermal Research*, *382*, 253–266. https://doi.org/10.1016/j.jvolgeores.2017.04.004

McNutt, S. R., & Roman, D. C. (2015). Volcanic Seismicity. In *The Encyclopedia of Volcanoes* (pp. 1011–1034). Elsevier. https://doi.org/10.1016/B978-0-12-385938-9.00059-6

Minakami, T. (1974). *Seismology of Volcanoes in Japan* (pp. 1–27). https://doi.org/10.1016/B978-0-444-41141-9.50007-3

Muslim, D., Sadisun, I., Nugraha, A. D., & Sekretariat, S. (2019). *Vulkanologi dan Bencana*. Kementerian Energi Dan Sumber Daya Mineral Republik Indonesia Badan Geologi.

Nugraini, L. D. A., & Safitri, D. A. (2023). Analisis Deformasi Gunung Agung Berdasarkan Data Citra SAR Sentinel-1A dan Metode D-InSAR. *Jurnal Ilmiah Geologi PANGEA*, *9*(1sp), 28. https://doi.org/10.31315/jigp.v9i1sp.9407

Nugroho, H., Widiyantoro, S., & Ibrahim, G. (2014). Penentuan Posisi Hiposenter Gempabumi dengan Menggunakan Metoda Guided Grid Search dan Model Struktur Kecepatan Tiga Dimensi. *Jurnal Meteorologi Dan Geofisika*, *8*(1), 48–60. https://doi.org/10.31172/jmg.v8i1.3

Octavia, D., Suharti, S., Murniati, Dharmawan, I. W. S., Nugroho, H. Y. S. H., Supriyanto, B., Rohadi, D., Njurumana, G. N., Yeny, I., Hani, A., Mindawati, N., Suratman, Adalina, Y., Prameswari, D., Hadi,

E. E. W., & Ekawati, S. (2022). Mainstreaming Smart Agroforestry for Social Forestry Implementation to Support Sustainable Development Goals in Indonesia: A Review. *Sustainability*, *14*(15), 9313. https://doi.org/10.3390/su14159313

Parwita, I. G. L. M., Mudhina, M., INTARA, I. W., & SUDIASA, I. W. (2019). Evaluasi Teknis Kinerja Bangunan Pengendali Lahar Tukad Unda Pasca Erupsi Gunung Agung Tahun 2017. *Construction and Material Journal*, *1*(1), 53–67. https://doi.org/10.32722/cmj.v1i1.1330

Pranata, B., Yudistira, T., Widiyantoro, S., Brahmantyo, B., Cummins, P. R., Saygin, E., Zulfakriza, Z., Rosalia, S., & Cipta, A. (2019). Shear wave velocity structure beneath Bandung basin, West Java, Indonesia from ambient noise tomography. *Geophysical Journal International*, *225*(3), 1850–1865. https://doi.org/10.1093/gji/ggz493

Pritaningtyas, A. D., Hasib, M., Kriswati, E., Indrastuti, N., & Zera, T. (2023). Analyses of explosion earthquakes at Sinabung Volcano: characteristics of waveform, spectra, and energy. *IOP Conference Series: Earth and Environmental Science*, *1227*(1), 012028. https://doi.org/10.1088/1755-1315/1227/1/012028

Sahara, D. P., Rahsetyo, P. P., Nugraha, A. D., Syahbana, D. K., Widiyantoro, S., Zulfakriza, Z., Ardianto, A., Baskara, A. W., Rosalia, S., Martanto, M., & Afif, H. (2021). Use of Local Seismic Network in Analysis of Volcano-Tectonic (VT) Events Preceding the 2017 Agung Volcano Eruption (Bali, Indonesia). *Frontiers in Earth Science*, *9*(1), 12034. https://doi.org/10.3389/feart.2021.619801

Suparman, Y., Syahbana, D. K., & Andreas, A. S. (2019). *Seismic Velocity Changes Associated with The 2017-2018 Activity of Mount Agung, Bali as Inferred from Cross-correlations of Ambient Seismic Noise (A Preliminary Result)*. https://doi.org/10.13140/RG.2.2.18249.08806

Syahbana, D. K., Kasbani, K., Suantika, G., Prambada, O., Andreas, A. S., Saing, U. B., Kunrat, S. L., Andreastuti, S., Martanto, M., Kriswati, E., Suparman, Y., Humaida, H., Ogburn, S., Kelly, P. J., Wellik, J., Wright, H. M. N., Pesicek, J. D., Wessels, R., Kern, C., … Lowenstern, J. B. (2019). The 2017–19 activity at Mount Agung in Bali (Indonesia): Intense unrest, monitoring, crisis response, evacuation, and eruption. *Scientific Reports*, *9*(1). https://doi.org/10.1038/s41598-019-45295-9

Wassermann, J. (2011). *Volcano Seismology*. https://doi.org/10.2312/GFZ.NMSOP-2_ch13

Wright, H. M. N., Pallister, J. S., McCausland, W. A., Griswold, J. P., Andreastuti, S., Budianto, A., Primulyana, S., Gunawan, H., Battaglia, M., Diefenbach, A., Griswold, J., Ewert, J., Kelly, P., Kern, C., LaFevers, M., Lockhart, A., Marso, J., Mayberry, G., McCausland, W., … Triastuty, H. (2019). Construction of probabilistic event trees for eruption forecasting at Sinabung volcano, Indonesia 2013–14. *Journal of Volcanology and Geothermal Research*, *382*(4), 233–252. https://doi.org/10.1016/j.jvolgeores.2018.02.003

Zulfakriza, Z., Nugraha, A. D., Widiyantoro, S., Cummins, P. R., Sahara, D. P., Rosalia, S., Priyono, A., Kasbani, K., Syahbana, D. K., Priambodo, I. C., Martanto, M., Ardianto, A., Husni, Y. M., Lesmana, A., Kusumawati, D., & Prabowo, B. S. (2020). Tomographic Imaging of the Agung-Batur Volcano Complex, Bali, Indonesia, From the Ambient Seismic Noise Field. *Frontiers in Earth Science*, *8*. https://doi.org/10.3389/feart.2020.00043